# Thermal effects on vortex breakdown in a swirling jet

J. Cohen[1] and D. Mourtazin[1]

## Summary

This experimental study shows that vortex breakdown (VB) can be effectively suppressed (enhanced) by prescribing a positive (negative) temperature difference between the surrounding fluid and the jet core. Moreover, the experimental critical swirl ratio for the appearance of VB is found to be in good agreement with a simple criterion, originally derived by [1] for isothermal swirling jets and extended here to include thermal effects.

## Introduction

VB is an intriguing phenomenon that can have detrimental effects (over delta wings at high angle of attack) or beneficial ones (as a flame stabilizer). Thermal effects on axisymmetric VB have been reported in various flow configurations, e.g. in a spherical gap [2] and in a container with a rotating bottom disk [3], where it was found that negative (positive) axial gradient of temperature can enforce (suppress) VB. In this article we extend the simple VB criterion, derived and experimentally verified by [1] for an isothermal swirling jet, to include thermal effects due to lateral temperature gradients. Our experimental results confirm the generalized criterion.

## A simple vortex breakdown criterion including thermal effects

Consider a free vortex undergoing conical breakdown in a flow of infinite extent (Fig. 1). The cylindrical coordinate system is used ($x$ ,$r$,$\theta$), where $x$ and $r$ are the axial and radial distances and $\theta$ is the azimuthal angle. The corresponding velocity components are ($V_x$, $V_r$, $V_\theta$). Applying the Bernoulli equation between two cross-stream planes, $X_1$ (close to the jet exit) and $X_2$ (the plane containing the stagnation point), along the centerline, and away from it where the ambient fluid is at rest, respectively yields:

$$P_{j_1} + \rho_j g H + 0.5\rho_j V_x^2(X_1,0) = P_{j_2}\,, \tag{1}$$

$$P_{amb_2} = P_{amb_1} + \rho_{amb} g H\,, \tag{2}$$

where P is the pressure, $\rho$ is the fluid density, g is the acceleration due to gravity and $H=X_2-X_1$ is the vertical distance between the two planes. The subscripts "j" and "amb" correspond respectively, to the jet and ambient fluid properties, whereas the subscripts "1" and "2" indicate the associated cross-stream planes.

[1] Faculty of Aerospace Engineering, Technion – Israel Institute of Technology, Israel

At the $X_1$ plane the radial pressure gradient is balanced by the centrifugal force:

$$P_{amb_1} = P_{j_1} + \int_0^\infty \rho_j \frac{V_\theta^2}{r} dr \,. \tag{3}$$

The radial density variation, due to the temperature difference between the ambient fluid and the jet ( $\Delta T = T_{amb} - T_j$ ), is approximated as

$$\rho_{amb} \approx \rho_j + \frac{\partial \rho}{\partial T}\Delta T = \rho_j(1 - \beta \Delta T); \quad \beta = -\frac{1}{\rho_j}\frac{\partial \rho}{\partial T}. \tag{4}$$

Finally, assuming $P_{j_2} = P_{amb_2}$ [1] and substituting Eqs. (2)-(4) into (1) leads to the following necessary condition for a vortex breakdown ($VB_{crit}$):

$$VB_{crit} = \frac{1}{V_x^2(X_1,0)} \int_0^\infty \frac{V_\theta^2}{r} dr - \frac{gH\beta\Delta T}{V_x^2(X_1,0)} \geq \frac{1}{2}, \tag{5}$$

where the inequality sign is applied to a bubble vortex breakdown configuration in which the stagnant zone is separated from the ambient quiescent fluid. In the following sections, this criterion is verified by experimental results.

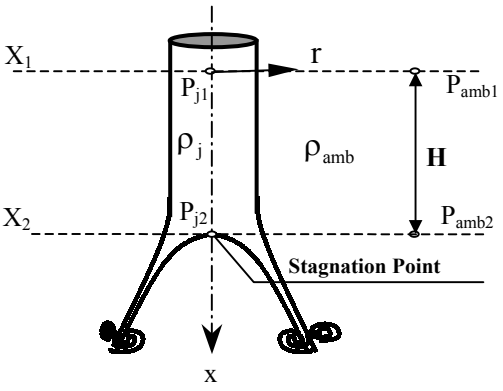


Fig. 1. Cone vortex breakdown.

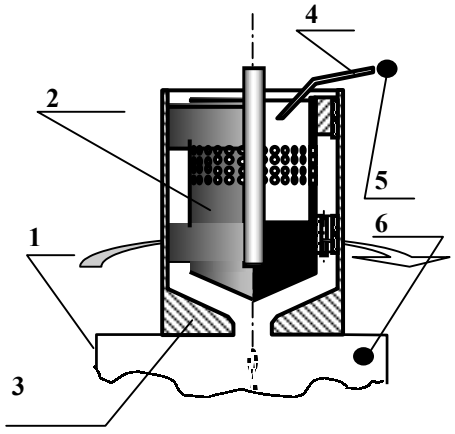


Fig. 2. Experimental setup.

## Experimental Setup

A schematic drawing of the apparatus is shown in Fig. 2. It consists of a vertical swirling jet discharging into a large cylindrical tank (1). The settling chamber (top part) is composed of a hollow inner perforated cylinder (2), having a conical end at its bottom, and an outer co-axial cylinder, connected to a

contracting nozzle (3) at its bottom. Water is supplied through three pipes (4) symmetrically positioned at the top of the inner cylinder. During the filling of the hollow inner cylinder, water flow through the network of holes to the gap separating the inner and outer cylinders. Then, the water flows downwards through a perforated ring before entering the nozzle part of the chamber. The jet exit diameter is 19.6 mm and the outer diameter of the test section is 226 mm.

Three independent parameters govern the flow: flow rate, fluid angular momentum and temperature difference between the ambient fluid and the jet. Closed loop water flow through the system is maintained by using a controlled pump. Swirl is imparted to the jet in the top contracting section through rotation of its outer part. During the experiments, the temperature of the ambient water in the cylindrical test section is kept constant at 296.6K using the room air-condition system. To control the temperature of the jet, the supplied water is passed through a copper coil immersed in a temperature-controlled bath. The bath temperature is calibrated against a T-type thermocouple (5) positioned at the entrance to one of the three water-supplying pipes. Two additional thermocouples positioned at the outer top part of the test section (6) and at its bottom exit, are used to monitor the ambient temperature during the experiments.

Particle Image Velocimetry (PIV) is utilized to measure the instantaneous and mean velocity fields in the (x, r) meridian plane. Laser Doppler Anemometry is used to obtain mean azimuthal velocity profiles along the radial coordinate.

## Results and discussion

The results presented here were obtained for a single Reynolds number of Re=247, based on the jet exit diameter and the average velocity there. The temperature difference between the ambient fluid and the jet was varied from (-4) ÷ (+6)K and the swirl number was varied continuously. Examples of the axial and azimuthal mean velocity profiles measured at $X_1$, for Re=247, $\Delta T$=4K and three values of $\Omega/\Omega_c$, where $\Omega$ is the angular velocity and $\Omega_c$ is its value when VB is initiated, are shown in Figs. 3a and 3b, respectively.

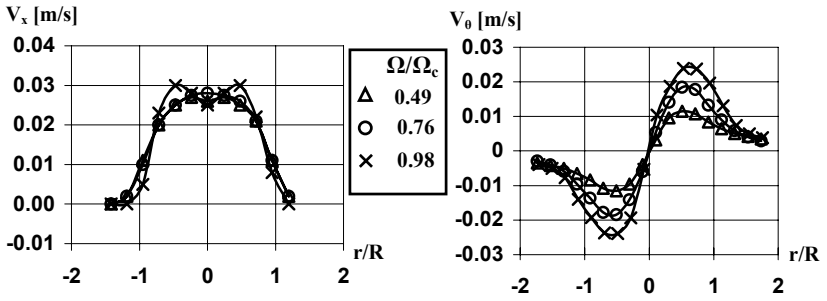


Fig. 3 Axial (a) and azimuthal (b) velocity profiles.

Vortex breakdown with bubble and conical shapes was obtained for positive and negative values of ΔT, respectively**.** For ΔT=0K the shape of the vortex was either a bubble or a cone. The prevailing shape at ΔT=0K was probably determined by the sign of the actually existing minute temperature difference.

The suppression of vortex breakdown is demonstrated in Fig. 4. Two PIV vector maps, obtained under the same flow conditions (Re=247,Ω=195 RPM) are shown. While a conical VB is evident for the isothermal case (Fig 4a), it is absent in Fig. 4b where ΔT=1K**.**

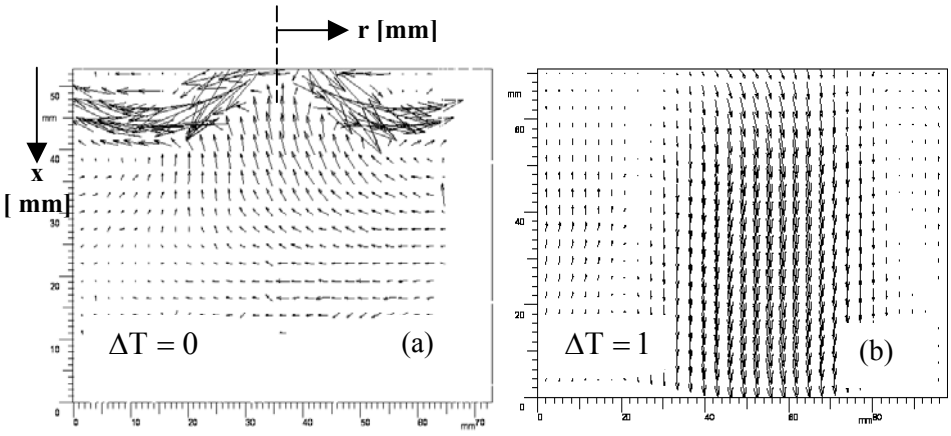


Fig. 4. PIV vector maps, $\Omega = 195$ RPM, $\mathrm{Re} = 247$.

In Figs. 5a-f, the temporal evolution of a conical vortex for ΔT=0K is shown. The elapsed time from the initiation of the stagnation point is indicated on each one of the figures. Initially, the stagnation zone is small and has a conical shape with a sharp apex angle (Figs. 5a-b). Then, a symmetrical bubble is formed (Fig. 5c), the size of which increases with time (Fig. 5d) until the bubble shape is transformed into a cone with a blunt apex angle (Figs. 5e-f). The height (H) between the stagnation point and the plane ($X_1$), located 3 mm downstream of the jet exit plane is indicated on Fig. 5a. This height, observed when the stagnation point is first initiated, is used to calculate the criterion (Eq. 5).

The theoretical necessary condition for VB (Eq. 5) was verified for Re=247 and several values of $\Delta T$. For each value of $\Delta T$, the jet swirl was increased by varying the outer cylinder rotation rate in small steps until a VB was initiated at $\Omega = \Omega_c$. The critical conditions for VB were calculated using $V_x(X_1,0)$ and $V_\theta(X_1,r)$ measured at $\Omega \approx 0.97\Omega_c$. The results are summarized in Fig. 6. It is evident that the onset of VB for all cases considered is slightly above the inviscid theoretical criterion, probably due to viscous effects.

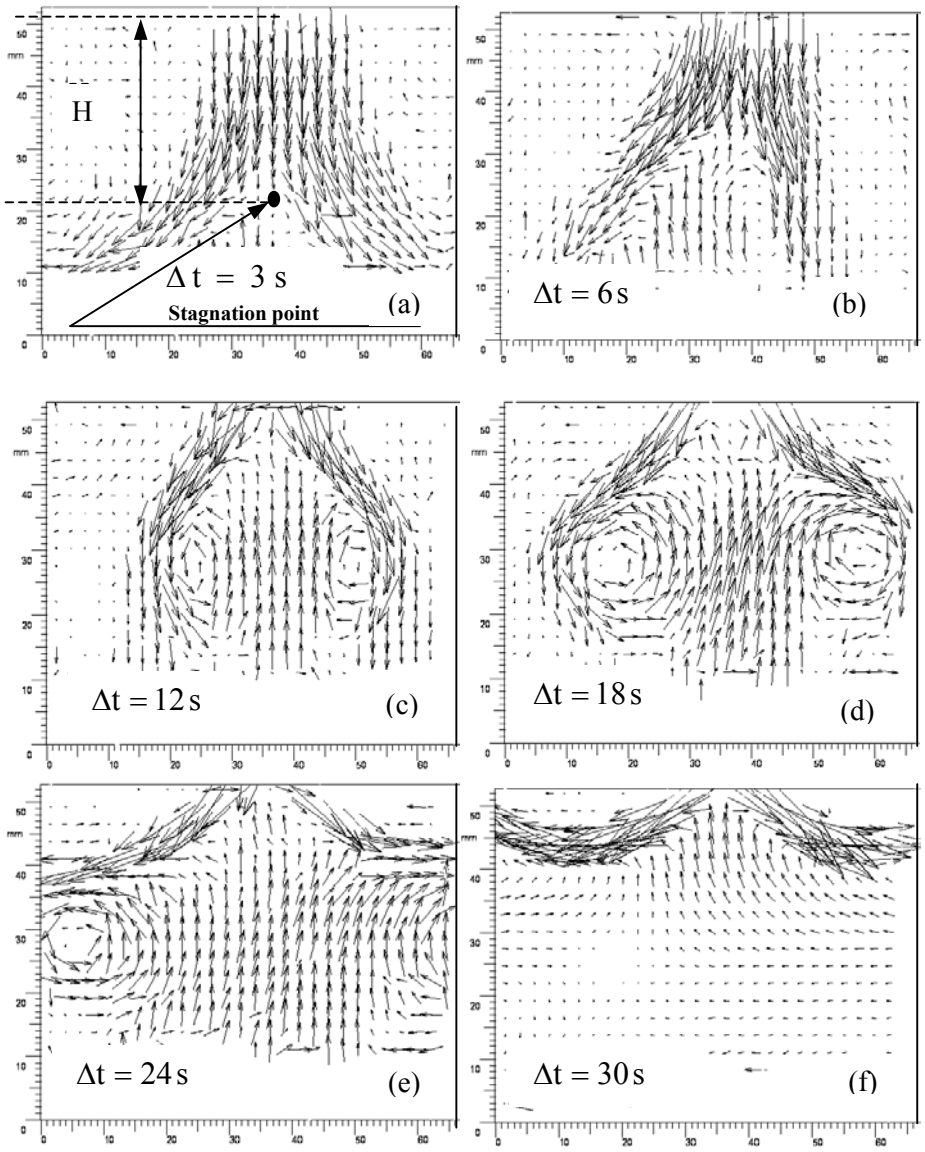


Fig. 5. Evolution of a conical vortex breakdown, Ω=195 RPM, ΔT=0K, Re=247.

Finally, a quantitative measure of the vortex breakdown suppression and enhancement is presented in Fig. 7. As the temperature difference is increased higher rotation rates are needed to initiate the vortex breakdown.

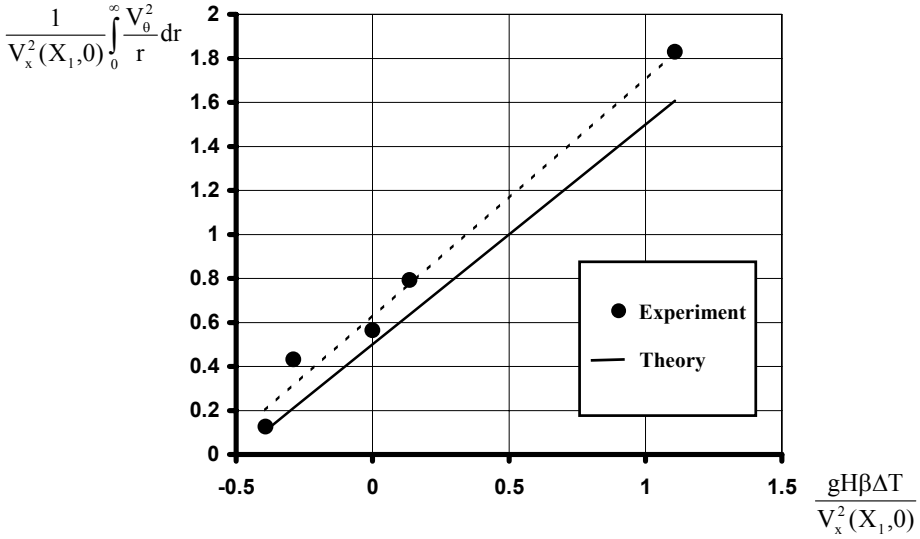


Fig. 6. Experimental verification of the theoretical criterion.

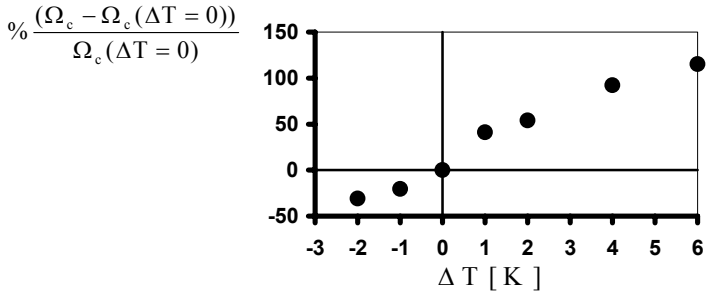


Fig. 7. Suppression/enhancement of the vortex breakdown.

## References

1. Billant, P., Chomaz, J.M. and Huerre, P. (1998): "Experimental study of vortex breakdown in swirling jets", *J. Fluid Mech*., Vol. 376, pp.183-219.
2. Arkadyev, A., Bar-Yoseph, P., Solan, A. and Roesner, K.G. (1993): "Thermal effects on axisymmetric vortex breakdown in a spherical gap", *Phys. Fluids*, A5(5), pp. 1211-1223.
3. Herrada, M.A., and Shtern, V. (2003): "Control of vortex breakdown by temperature gradient", *Physics of Fluids*, Vol.15, pp. 3468-3477.